Food Hydrocolloids 104 (2020) 105692

Contents lists available at ScienceDirect

Food Hydrocolloids

journal homepage: http://www.elsevier.com/locate/foodhyd

Tribology and rheology of bead-layered hydrogels: Influence of bead size on sensory perception

Ecaterina Stribiţcaia, Emma M. Krop, Rachel Lewin, Melvin Holmes, Anwesha Sarkar *

Food Colloids and Bioprocessing Group, School of Food Science and Nutrition, University of Leeds, Leeds, LS2 9JT, United Kingdom

ARTICLE INFO

Keywords:
Soft beads
Particle size
Friction coefficient
Viscosity
Sensory discrimination
Oral tribology

ABSTRACT

The aim of this study was to understand the influence of the size of soft beads embedded in layered hydrogels on mechanical performance as well as sensory discrimination and perception. Layered hydrogels were designed using a monolayer of calcium alginate (CaA) beads of small, medium and large size (diameter of 805, 1413 or 1725 μm, respectively) sandwiched in between layers of *kappa*-carrageenan (κC) gel matrix, with controls created using pure κC hydrogels and κC + sodium alginate (NaA) mixed gels. Large deformation rheology of the hydrogels followed by apparent viscosity as well as tribological properties of the hydrogel boli (after homogenising with simulated saliva) were analysed. Sensory discrimination tests (n = 113) and intensity ratings (n = 60) were conducted with untrained panellists. Bead size did not have an influence on the rheological properties of the layered hydrogels and hydrogel boli, respectively ($p > 0.05$). However, the lubrication behaviour of the layered hydrogel boli was influenced by bead size, with gels containing large-sized beads showing highest lubrication in both boundary and mixed regimes ($p < 0.05$). Although panellists were able to discriminate non-layered gels from bead-layered counterparts based on textural attributes, such as "hard", "chewy" and "pasty", they could not distinguish between small and large-sized bead-layered gels in contrast to the oral tribology results. The low modulus of the beads appeared to be the limiting factor to detect differences based on bead sizes in this study. Findings on instrumental characterization and consumer perception of bead-layered hydrogels can have important implications for development of novel food texture.

1. Introduction

Foods in general are heterogeneous composite structures with particles of various sizes, shapes and viscoelastic moduli embedded in complex polysaccharide and protein networks. Examples of such composite foods may range from the conventional use of freeze-dried fruit pieces in porridge and yoghurt, and starch granules in custards to the more recent usage of flavoured gelatine pearls in confectionery, pieces of cookies in ice creams and seeds/nuts inclusion in cheese, *etc.* Indeed such interesting inclusions of particles are increasingly enabling novel texture creations and triggering hedonic escalation of these palatable foods. In addition to creating new hedonic textural experiences, there is an increasing body of evidence showing texturally complex foods containing inclusions can influence oral processing behaviour in human subjects (Krop, Hetherington, Miquel, & Sarkar, 2019c; Santagiuliana, Christaki, Piqueras-Fiszman, Scholten, & Stieger, 2018a; Santagiuliana, Piqueras-Fiszman, van der Linden, Stieger, & Scholten, 2018b). These complex foods containing particle inclusions have shown the ability to reduce food intake and so offer a contributory element toward the global obesity challenge (Krop, Hetherington, Miquel, & Sarkar, 2019b; Krop et al., 2018; Larsen, Tang, Ferguson, & James, 2016a; Tang, Larsen, Ferguson, & James, 2016). In addition, manipulating texture by incorporation of soft gel particles in model foods such as hydrogels has been shown to increase the oral residence time during oral processing experiments in elderly population cohorts, without necessarily altering the large deformation properties of the gels (Laguna, Hetherington, Chen, Artigas, & Sarkar, 2016a; Sarkar, 2019). Thus, research into model and real foods with textural complexity particularly with embedded inclusions will increase the understanding of sensory and functional relationships during oral processing and contribute toward the two key global challenges of obesity and healthy ageing.

Conventionally, hard particles in gel networks have been used to study the effect on oral sensation, where even 10 μm-sized alumina particles have been shown to cause sensory 'grittiness' (Utz, 1986). Interestingly, in another study 230 μm-sized spherical deformable polystyrene particles were perceived to be smaller than that 80 μm-sized

* Corresponding author.
E-mail address: A.Sarkar@leeds.ac.uk (A. Sarkar).

https://doi.org/10.1016/j.foodhyd.2020.105692
Received 14 October 2019; Received in revised form 14 January 2020; Accepted 20 January 2020
Available online 23 January 2020

irregular, hard silica particles (Engelen, Van der bilt, Schipper, & Bosman, 2005). Both modulus and shape of the particles are highly relevant in textural perception, such that sharp-faceted hard particles tend to have a lower threshold to be perceived easily than the relatively soft spherical particles (Tyle, 1993). Such findings have later been shown to be related to friction, with spherical particles having significantly lower friction than particles with sharp facets (de Wijk & Prinz, 2005; Liu, Tian, Stieger, van der Linden, & van de Velde, 2016; Sarkar, Kanti, Gulotta, Murray, & Zhang, 2017). In addition, the matrix in which the particles are dispersed can also play a key role in oral sensation, for example, depending on the variety of cheese in which cellulose particles were embedded, the threshold size of microcrystalline cellulose ranged from 52 to 86 μm (Santagiuliana et al., 2019).

Recently, the focal point in studying textural complexity has shifted from studying the inclusion of hard particles to soft polymeric gel particles. For instance, Laguna and Sarkar (2016) demonstrated that the inclusion of soft calcium alginate beads can generate structural defects in carrageenan-based hydrogels affecting oral processing behaviours, such as the number of chews and swallowing time by using a range of large deformation rheological characterizations and sensory analyses using a trained panel. Krop, Hetherington, Holmes, Miquel, and Sarkar (2019a) further highlighted that the presence of 1000 μm-sized calcium alginate gel beads can not only affect the bulk rheological properties, but also influence the tribological properties of the hydrogel boli, with the latter affecting lubrication-related sensory attributes such as “pasty”, “smooth” and “melting” as compared to the non-beaded mixed sodium alginate-carrageenan gels. In another recent work, Santagiuliana et al. (2018a) studied the impact of the particle size of κ-carrageenan gel beads varying in size (0.8–4.2 mm) on the large deformation properties and sensory perception of proteins gels and soups, however tribological properties were not investigated in this study. Noteworthy, in these studies by Krop et al. (2019a) and Santagiuliana et al. (2018a) the beads were uniformly dispersed throughout the hydrogel matrix and it was not possible to identify whether the beads had been displaced from the hydrogels matrix during oral processing or if they were still associated even if they were “inactive fillers”.

Hence, it is important to understand how the instrumental and sensorial response of these hydrogels with polymeric gel particle inclusions might alter if the gel particles were present as “layers” rather than being incorporated homogeneously in the matrix. Although effect of bi-layer food gels has been investigated by Santagiuliana et al. (2018b) and Devezeaux de Lavergne, van de Velde, van Boekel, & Steiger (2015) on the textural perception and sensory profile, to our knowledge, layered hydrogels incorporating soft polymer beads has not been reported in literature and a fundamental understanding of the rheological, tribological and sensory profiles of such complex hydrogels and the effect of size of the embedded soft beads remains to be elucidated.

Soft tribology analyses determining the lubrication and friction of oral surfaces in relative motion using polymeric substrates is progressively becoming a useful mechanical technique to understand the physical mechanism behind perceived texture (Pradal & Stokes, 2016; Sarkar, Andablo-Reyes, Bryant, Dowson, & Neville, 2019a; Stokes, Boehm, & Baier, 2013). The use of model saliva (also referred to as artificial saliva) in previous literature by Sarkar, Goh, and Singh (2009) has been observed to further strengthen the correlation with sensory attributes, however only few studies have used this to simulate realistic oral processing conditions (Sarkar & Krop, 2019b). Hence, it is crucial to combine traditional rheological measurements with tribological analyses to comprehend the mechanical phenomena behind sensory perception.

Therefore, the aim of this study was to investigate textural complexity in terms of the size of soft polymeric beads in layered hydrogels using instrumental characterization with and without simulated oral processing and identify whether such textural properties attributed to different bead sizes can then be sensorially discriminated and perceived by consumers (untrained panellists). We hypothesize that consumers will be able to discriminate layered from non-layered hydrogels and also distinguish samples based on bead size, which can be explained by the intensity ratings of the textural attributes and the tribological behaviour of the samples.

2. Materials and methods

2.1. Materials

Food grade kappa-carrageenan (κC), sodium alginate (NaA) and watermelon flavouring were purchased from Special Ingredients Ltd (Chesterfield, UK). Watermelon food colouring was purchased from AmeriColor Corp. (Placentia, California USA). Stevia granulated sweetener was purchased from a local supermarket (Leeds, UK). Food grade potassium chloride (KCl) was purchased from Minerals Water Ltd. (Purfleet, UK) and calcium chloride dehydrate ($CaCl_2.2H_2O$) was obtained from VWR Chemicals (Leuven, Belgium). All chemicals used to prepare the model saliva: sodium chloride (NaCl), potassium dihydrogen phosphate (KH_2PO_4), potassium citrate ($K_3C_6H_5O_7.H_2O$), uric acid sodium salt, urea ($C_5H_3N_4O_3Na$), lactic acid sodium salt ($C_3H_5O_3Na$) and porcine gastric mucin Type II, were purchased from Sigma-Aldrich (Dorset, UK). All materials were used without further purification. Distilled water was used to prepare both the hydrogels and model saliva.

2.2. Preparation of hydrogels

The composition of the hydrogels used in this study is shown in Table 1. A batch of 200 mL of each of the gel samples was prepared in a bottle and transferred into a petri-dish to a height of 10 mm (150 g gel in each of the petri-dishes, diameter: 140 mm), and then kept at 4 °C overnight to set. The hydrogels were prepared in at least three replicates and cut from the petri-dish using a circular-cutter (diameter of 25 mm and 5.6 g in weight) or a heart-shaped cutter (largest dimensions of 15 mm horizontally and 14 mm vertically, respectively and 1.7 g weight). The heart shape was used for the sensory evaluations to increase sample acceptability as determined during pilot testing with these model gels.

2.2.1. Kappa-carrageenan (κC) hydrogels

Firstly, 0.02 M KCl solution was prepared and 0.5 wt% of the sweetener was added and stirred until it was completely dissolved. Appropriate quantities of κC (see Table 1) were added to the sweetened KCl solution and mixed for 30 min on a magnetic stirring plate. Once the κC was hydrated, the polymer solution was heated to 90 °C in a shaking water bath at 80 rpm (OLS26, Aqua Pro, Grant Instruments, Royston, UK), for at least 60 min until it was completely dissolved. Then 0.5 wt% of the watermelon flavouring and 0.5 wt% of the diluted food colouring (2 wt%) was mixed into the κC gel mixture, before being allowed to set in the petri-dishes at 4 °C overnight.

Table 1
Composition of the hydrogels.

Hydrogel samples[a]	κC (wt%)	NaA (wt%)	CaA beads (wt%)	Water (wt%)
2κC	2.00			96.50
1.67κC + 0.33NaA	1.67	0.33		96.50
1.67κC + 0.33CaA$_{Small}$	1.67		0.33	96.50
1.67κC + 0.33CaA$_{Medium}$	1.67		0.33	96.50
1.67κC + 0.33CaA$_{Large}$	1.67		0.33	96.50

[a] All hydrogels also contained 0.5 wt% watermelon flavouring, 0.5 wt% diluted colouring and 0.5 wt% sweetener. The CaA beads were prepared from a 1 wt% NaA solution and the final total hydrocolloid composition was achieved by layering of 2.5 wt% κC solution and 1 wt% CaA beads (2:1).

2.2.2. Kappa-carrageenan + sodium alginate (κC + NaA) hydrogels

Mixed κC + NaA hydrogels were prepared using appropriate quantities of κC and NaA in 0.02 M KCl solution containing sweetener (as described above). The mixture was stirred for 30 min until it was fully hydrated. The polymer solution was then heated to 90 °C in a shaking water bath at 80 rpm, for at least 60 min until it was completely dissolved. The mixed gelling solution was then removed from the water bath, and 0.5 wt% the flavouring and colouring was mixed into the κC + NaA solution before being allowed to set in the petri-dishes at 4 °C overnight.

2.2.3. Layered kappa-carrageenan + calcium alginate hydrogels (κC + CaA)

The κC + CaA layered hydrogels consisted of CaA beads of different sizes, these beads were incorporated as a sandwiched layer between two distinct layers of κC gel. The CaA beads were prepared by extruding 1 wt % NaA solution through a vibrating nozzle of either 150, 300 or 450 μm (Buchi Encapsulator B-390®, Buchi UK Ltd, Chadderton, UK) into a beaker containing 0.01 M $CaCl_2$ under constant stirring at 300 rpm to prevent aggregation of the CaA beads. A frequency of 500 Hz and electrode setting of 1500 V were used, and, depending on nozzle size, the air pressure varied from 250 to 750 mbar to achieve a constant flow of the NaA droplets. After stirring for 20 min, the CaA beads were collected by filtration (Whatman™ filter paper, Grade 1, 185 mm diameter, Buckinghamshire, UK). The beads were then washed three times using distilled water to remove any residual $CaCl_2$. The layered hydrogels were prepared by pouring 50 g of 2.5 wt% κC solution containing the sweetener, flavouring and colouring (prepared as mentioned above) into a petri-dish and leaving to set for approximately 5 min. Then, a layer of 50 g of CaA beads of processing size of 150, 300 or 450 μm was added. Finally, another layer of 50 g of κC solution was transferred onto the top of the layer of beads, sandwiching the layer of beads between the two κC layers and resulting in a total biopolymer concentration of 2 wt%. The petri-dish was left to set at 4 °C overnight.

2.3. Optical microscopy

The prepared CaA beads were analysed using a microscope (Nikon SMZ-2T, Japan) to determine the actual size of the beads generated by the Buchi Encapsulator B-390®. The CaA beads were carefully placed on a glass slide and 0.1 mL of distilled water was added on top of the beads to avoid dehydration and shrinkage of the beads. Using a magnification of 4 ×, images showing the full outline of the spherical individual beads were captured. This was repeated for approximately 75 individual beads from each nozzle size. The ImageJ software (version 1.48r, National Institute of Health, Bethesda, USA) was used to determine the diameter of the different beads and the mean bead size was calculated for the different processing nozzles.

2.4. Large-strain compression

Both uniaxial single compression tests and puncture tests were carried out on each of the five hydrogels using a TA-TX2 Texture Analyser (Stable Micro System Ltd., Surrey, UK) attached with a 50 kg load cell. A cylindrical 59 mm platen probe was used for the compression tests (Stable Micro Systems Ltd., Surrey, UK), which were performed at room temperature (22 °C) at a deformation level of 80% strain and a constant speed of 1 mm s^{-1}. Gel samples were cut from each of the petri-dish using the circular cutter (25 mm diameter). At least six repetitions were performed for each of the hydrogel cut-outs from at least two different preparation days. The force-distance curves obtained from each test were recorded using the Exponent software (TEE32, v6.1.9.0, Stable Micro Systems Ltd., Surrey, UK). The data from the force-distance curves were converted into stress-strain curves, and the maximum peak of the curve was used to determine the gel's fracture point.

For the puncture tests, a Volodkevitch Bite Jaw probe (Stable Micro Systems Ltd., Surrey, UK) was used, with the same parameter settings. The fracture force (N) of the hydrogels was determined directly from the peak of the obtained force-distance curves. At least six repetitions were performed for each of the hydrogels from at least two different preparation days.

2.5. Preparation of artificial saliva

The model saliva was prepared following the composition previously described by Sarkar et al. (2009), except ammonium nitrate was excluded. Briefly, to prepare 1 L of model saliva, 1.59 g L^{-1} NaCl, 0.64 g L^{-1} KH_2PO_4, 0.20 g L^{-1} KCl, 0.31 g L^{-1} $K_3C_6H_5O_7.H_2O$, 0.02 g L^{-1} $C_5H_3N_4O_3Na$, 0.20 g L^{-1} H_2NCONH_2, 0.15 g L^{-1} $C_3H_5O_3Na$ and 3.00 g L^{-1} porcine gastric mucin type II were dissolved in distilled water. After adjusting the pH to 7.0 using 1 M NaOH, the volume was made up to 1 L using a volumetric flask. Porcine gastric mucin was used to prepare the model saliva to have a comparison with previous studies (Krop et al., 2019a; Torres et al., 2019) and due to the ability of this mucin to simulate the rheological properties of human saliva. It is noteworthy, however, that bovine submaxillary mucin is the optimal source of commercially available mucin for lubricating properties (Sarkar, Xu, & Lee, 2019c), and therefore this is a limitation of the current study. In addition, α-amylase was not included in the model saliva formulation as starch was not used in any of the hydrogels tested and therefore, the role of α-amylase was considered to be negligible as seen in previous literature dealing with non-starch polysaccharides (Torres et al., 2019).

2.6. Preparation of simulated hydrogel boli

For the viscosity and tribology measurements, hydrogel boli were generated to simulate oral processing by mixing the various hydrogels or CaA beads alone with model saliva at 4:1 w/w ratio based on previous literature (Devezeaux de Lavergne, van de Velde, van Boekel, & Stieger, 2015). About 160 g of hydrogels (twenty-eight circular hydrogel cut outs) were mixed together in a food blender (Andrew James UK Ltd., Bowburn, UK) with 40 g of simulated saliva for 20 s at the lowest speed setting (speed 1) (Krop et al., 2019a).

2.7. Apparent viscosity

The apparent viscosity of the hydrogel boli in the presence of model saliva was measured with a rheometer (Kinexus Ultra+, Malvern Instruments Ltd, Worcestershire, UK) using a plate-plate geometry (diameter 60 mm). For the 2κC boli a gap size of 1 mm was used, whereas for the other gel boli samples the gap size was 0.5 mm, adjusting for the hydrogels' bead sizes once broken down. The samples were sealed off with a thin layer of silicone oil to prevent evaporation. Flow curves were obtained for all hydrogel boli after simulated oral processing at shear rates ranging from 0.01 to 1000 s^{-1} at 37 °C. A minimum of three replicates were measured for each hydrogel sample.

2.8. Tribology

Soft tribology measurements of MilliQ water, 1 wt% NaA solution, CaA beads alone, model saliva, CaA beads boli (*i.e.* CaA beads + model saliva) and hydrogel boli (*i.e.* hydrogels + model saliva) were carried out using a MTM2 Mini-Traction Machine (PCS Instruments, UK). Polydimethylsiloxane (PDMS) ball (diameter of 19 mm, MTM ball Slygard 184, 50 Duro, PCS Instruments, London, UK) and disc (diameter of 46 mm, thickness of 4 mm) were used for the measurements (surface roughness of PDMS tribopairs, $R_a < 50$ nm). Approximately 30 g of sample was loaded onto the pot equipped with the PDMS disc; the ball was lowered onto the disc and then the pot was covered with a lid. The entrainment speed was decreased from 0.3 to 0.001 m s^{-1}, and the friction coefficients were recorded at slide-roll-ratio of 50% at 2 N load with a Hertzian contact pressure of ~200 kPa (Sarkar et al., 2019a). The

temperature was set and maintained at 37 °C, to imitate the temperature at which oral processing occurs. A minimum of three repetitions were carried out for each sample.

In order to understand the role of the bulk rheological properties on tribology, Stribeck curves were plotted showing the evolution of friction coefficient as a function of the product of the entrainment speed component (U) and the shear rate viscosity (η) at 1000 s^{-1} of the simulated hydrogel boli of 2κC, 1.67κC+0.33CaA_{Small} and 1.67κC+0.33CaA_{Large} with MilliQ water as a reference.

2.9. Discriminative and sensory ratings tests

Two types of sensory tests were carried out: a discriminative test and a descriptive test. The sensory trials were approved by the Faculty Research Ethics Committee of the University of Leeds (MEEC-16-046) and all participants were required to read a participant information sheet and sign a consent form before taking part in the study. At the end of the test, the participants were reimbursed for their participation.

A total of 113 untrained panellists, 42 males and 71 females (ranging 20–55 years, mean age 28.8 ± 7.8 years), participated in triangle tests involving the κC + NaA and 150, 300 and 450 μm layered κC + CaA hydrogels. In each triangle, the participant received a set of three hydrogels, two identical and one that was different. A randomisation order was generated using the CompuSense software (v5.0, Ontario, Canada). The samples were placed in small, clear plastic sampling cups, labelled with a random three-digit codes. Participants were seated in individual sensory booths, set up with red lighting to avoid panellists being able to visually distinguish between the hydrogel samples before consuming them. Participants were asked to collect the samples from the cup using a teaspoon, to chew each sample as they would normally do, going from left to right in the presented order of samples, and then to identify the anomalous sample. Answers to each triangle test were recorded on a paper questionnaire. Participants were encouraged to sip water and consume cracker (Jacob's Cream Crackers, Jacob's Bakery, Leicestershire, UK) between each triangle test, to cleanse the oral palate and ensure accurate sensory perception in each of the triangle tests.

Besides the discriminative test, 60 participants (24 males, 36 females, mean age 30.4 ± 8.0 years) took part in a rating test where they were asked to rate the mixed and bead-layered hydrogels compared to a reference sample for six different texture attributes (see Table 2) that were determined to be relevant based on a previous study using similar types of κC-based hydrogels (Krop et al., 2019a). The attribute 'gritty' was included based on previous literature dealing with different sizes of hydrogel beads (Santagiuliana et al., 2018a). The four samples were presented in randomised order in a balanced block design. The intensities of the attributes were rated on an unstructured line scale of 100 mm, anchored from 'not at all' (0 mm) to 'extremely' (100 mm), as compared to 2κC (the reference sample) of which the intensity scores were provided (see Table 2). The reference sample was tasted first and provided again to the participants at any time during the sensory evaluations upon request. The scores for the reference sample were already filled out on the rating scales for all the attributes (see Supplementary Fig. S1). Participants were asked to place the whole sample in their mouth and chew, after which they were presented with two options – either to swallow the sample or to expectorate the samples in the provided cups if they felt inclined to do so. Between the samples, panellists were instructed to rinse their mouth with some water and to consume cracker to cleanse their palate. Data was recorded using CompuSense software (v5.0, Ontario, Canada) and exported for analysis.

Table 2
Texture attributes used in the sensory ratings tests with a short description. In between brackets the score for the 2κC reference sample are shown.

Texture attributes	Definitions
Hard	The force needed to compress the sample between the tongue and the palate (100 mm).
Chewy	The amount of chews needed to break down the sample to be ready for swallowing (100 mm).
Smooth	Absence of abrasiveness/resistance of the products' surface as perceived by the tongue or palate (100 mm).
Slippery	The ease in which the sample slides through the mouth during chewing and slips away from the teeth (100 mm).
Pasty	The sensation of the presence of wet/soft (immiscible) solids in the mouth *i.e.* muddy (0 mm).
Gritty	The presence of small hard particles that stick to the teeth/palate *i.e.* presence of residues (0 mm).

2.10. Statistical analysis

Mean values and standard deviations (SD) were calculated using Microsoft® Excel (Microsoft Office Professional Plus 2016; Microsoft Corporation), and data was plotted using the software Origin® (OriginPro 2018; OriginLab Corporation, Northampton, USA). Differences between measured bead size, puncture force and compression fracture strain of hydrogels, coefficients of friction of hydrogel boli, beads boli and beads alone in the boundary and mixed lubrication regimes were determined by analysis of variance (one-way ANOVA). Least significant differences were calculated by Bonferroni's post-hoc tests. Statistical significance was set at $\alpha < 0.05$ level.

For the sensory discrimination test, the significance was determined for each triangle test separately due to the variation in total number of participants that completed each test. For the sensory intensity ratings, the panel performance was checked by evaluating the variance as well as identification of any potential outliers in the data. To check for differences in the sensory intensity ratings between hydrogels, non-parametric repeated measure Friedman tests were applied with post-hoc pairwise multiple comparison tests according to Nemenyi (1963). To check for correlations between sensory attributes, Pearson correlations were computed. All statistical analyses were done using SPSS (IBM® SPPS® Statistics, v25, SPSS Inc, Chicago, USA) or R version 3.5 (R Core Team, 2018, p. 2012), and the significance level was set at $\alpha < 0.05$.

3. Results and discussion

3.1. Characteristics of the CaA beads

3.1.1. Characterization of bead size

CaA beads of varying sizes were prepared using the three different vibrating nozzles with processing sizes of 150, 300 and 450 μm in order to generate textural complexity in the hydrogel matrix. High-resolution optical microscopy images confirmed that the encapsulator was producing spherical beads, as desired (see Fig. 1). Qualitatively, comparing the beads shown in the optical micrographs in Figs. 1ai-ci, one can easily appreciate that there is a clear difference in the diameter of the beads depending on the type of nozzle (150–450 μm diameter) used. For instance, Fig. 1ai shows four entire beads, while Fig. 1bi shows only one of them and in Fig. 1ci, even a single bead could not be fitted within the microscopic view.

Quantitatively, the size distribution of at least 75 individual beads for the three groups of CaA beads are displayed in histograms (Fig. 1aii-cii). The average diameter calculated from the images obtained through microscopy were notably different from the nozzle diameter. The 150 μm nozzle produced small beads with an average diameter of 805 μm (Fig. 1aii), the 300 μm nozzle formed medium-sized beads with an average diameter of 1413 μm (Fig. 1bii), and the 450 μm nozzle produced large beads with an average diameter of 1725 μm (Fig. 1cii). Although distinctively different in size from each other ($p < 0.05$), the beads were considerably larger than expected. Such increase in size could be explained by the fact that the beads were rather soft with elastic modulus ranging from 0.1 to 1.0 kPa (Mahdi, Diryak, Kontogiorgos, Morris, & Smith, 2016) and thus, these

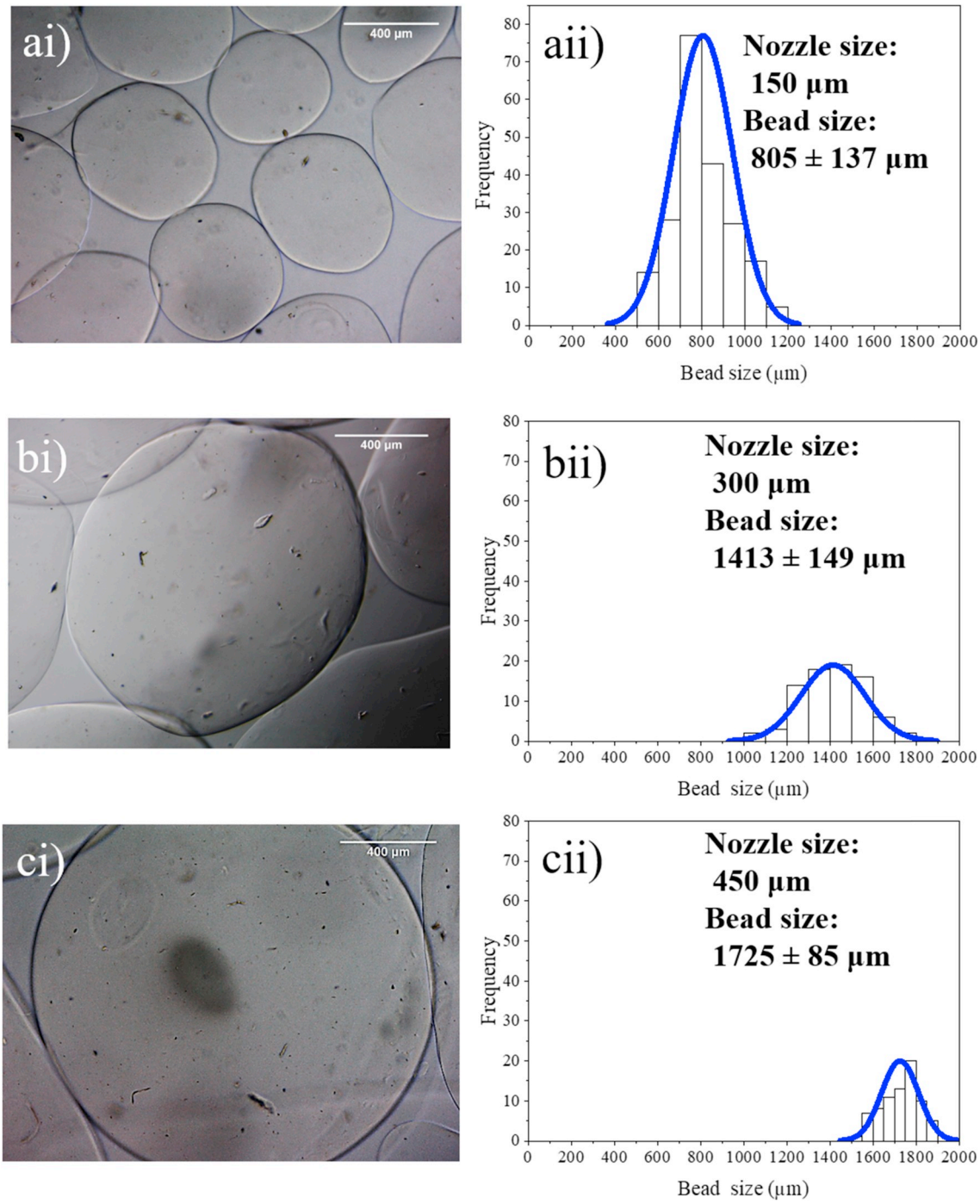

Fig. 1. Optical micrographs (i) and histogram with log-normal fitting (blue solid line) of the bead size distribution (ii) of 1 wt% CaA beads synthesised using the Buchi Encapsulator® with 150 µm (a), 300 µm (b), and 450 µm (c) sized nozzle, producing small, medium and large beads, respectively. Based on the microscopy images of at least 75 beads, the actual mean diameter of the beads was assessed using ImageJ. Each bead size differed significantly from each other: $p < 0.05$. Scale bars represent 400 µm. (For interpretation of the references to colour in this figure legend, the reader is referred to the Web version of this article.)

beads can be hypothesized to become flat 'pancake'-shaped when interacting with the glass slide during microscopy analysis. One might also expect such beads to be flattened in the mouth when such beads interact with the tongue surface, with modulus of the tongue/palate (2.5 kPa) and oral contact pressure (30–70 kPa) being higher than the modulus of the beads (Sarkar et al., 2019a). Another possible reason for the increase in size is that these beads might have been swollen in the presence of buffer, increasing their volume, which can also occur *in vivo* upon interaction with human saliva.

3.1.2. Tribological behaviour of the CaA beads

It is likely that during oral processing of the layered hydrogels the CaA beads might be expelled from the hydrogel matrix. Hence, the tribological properties of the CaA beads on their own were first characterised by plotting the friction coefficient values against the entrainment speeds. Fig. 2 shows the friction coefficient curves for each of the different CaA beads, 1 wt% NaA solution and MilliQ water and a general trend in reduction of friction coefficients in the direction of the applied entrainment speed ramp. The friction coefficient curve for the NaA solution serves as a control for the beads to understand if the friction

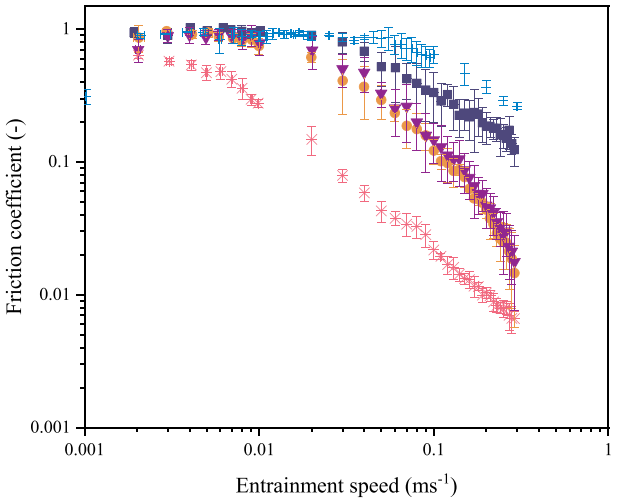

Fig. 2. Mean friction coefficient of MilliQ water (–), 1 wt% NaA solution (x) and CaA beads - small (■), medium (●) and large (▼) as a function of entrainment speed at 37 °C, respectively. The mean was calculated based on at least three replicates. Error bars show the standard deviation.

behaviour is dominated by the bursting of the CaA beads or if the beads remain relatively intact in the contact zone where the PDMS contact pressure in the tribometer (~200 kPa) can be expected to be two orders of magnitude higher than that of the alginate gel beads (Sarkar et al., 2019a). Irrespective of the size of the beads, all the CaA bead curves as well as NaA solution curve demonstrated boundary and mixed lubrication regimes because the speeds were varied in the orally relevant speed range of 0.001–0.300 m s^{-1} (Fig. 2), and therefore a hydrodynamic regime was not expected in this low speed range.

In the boundary regime, where the entrainment speed is at its lowest (≤0.01 m s^{-1}), the friction coefficient values for all the CaA beads of three different sizes appeared to be very similar ($p > 0.05$) (see Supplementary Table S1a for statistics). The micron-sized CaA beads were too large in size to enter the contact region and reduce the friction coefficients between the PDMS ball and disc, where the contact radius is generally expected to allow only a few molecules to nanometer thick layers of lubricating materials. This is further evidenced by the CaA beads having a similar boundary friction profile to MilliQ water (Fig. 2), and thus the beads were possibly excluded from the hydrophobic PDMS-PDMS contact region until the curves shifted from boundary to a mixed lubrication regimes allowing the CaA beads to be entrained. Such behaviour has also been seen previously in starch-based hydrophilic microgel particles, where microgels of ≥30 μm were unable to enter the contact zone in the boundary regime (Torres, Tena, Murray, & Sarkar, 2017) or in case of agarose fluid gels where particles were not entrained in PDMS-PDMS contact unless the critical sliding speed was reached (Gabriele, Spyropoulos, & Norton, 2010). It can be noted that the friction coefficients of the NaA solution were significantly lower than those of CaA beads irrespective of the entrainment speeds (Supplementary Table S1a). This suggests that although hydrophilic NaA might not be expected to be adsorbed to hydrophobic PDMS surface, NaA with a radius of gyration of ~50 nm may be able to enter the contact and provide some boundary lubrication properties (Strand, Bøe, Dalberg, Sikkeland, & Smidsrød, 1982).

The friction coefficient of the CaA beads and NaA solution decreased with increasing entrainment speed at > 0.01 m s^{-1} to 0.3 m s^{-1} (Fig. 2), indicating that all these samples at these conditions were in the mixed lubrication regime of the friction curves. As can be expected from the difference in the nanometric sized layers of NaA solution and the hundreds of micron-sized CaA beads, NaA solution expectedly accelerated the onset of the mixed lubrication regime (<0.01 m s^{-1}) as compared to that of the bead dispersions. In the mixed regime, particularly ≥0.1 m s^{-1}, the CaA beads (medium and large) showed significantly lower friction coefficients as compared to that of the small CaA beads ($p < 0.05$) (Supplementary Table S1a). The trend of friction coefficient values with increasing bead sizes was small > medium ≈ large, *i.e.* higher lubricating properties correlated with larger bead sizes.

It is worth noting that the Young's modulus of gel beads may scale inversely with the particle volume *i.e.* cubed function of the particle diameter (Hashmi & Dufresne, 2009). The CaA beads have a very low modulus (≤1.0 kPa) (Mahdi et al., 2016), and consequently, the large-sized CaA beads can be anticipated to have an order of magnitude lower modulus as compared to that of the small-sized beads $\left((Diameter_{CaA_{small}})^3 \Big/ (Diameter_{CaA_{large}})^3 \right) \approx 0.1$ (see Fig. 1 for mean bead size diameter). It is thus possible that the medium and large beads were able to entrain, easily deform in shape and flatten to fit in the contact zone between the ball and disc and were capable of efficiently separating the tribo-surfaces, as has been observed in a previous study using micron-sized starch-based microgels (Torres et al., 2017). Another possibility is that due to their extremely low moduli, the large and medium-sized CaA beads were compressed to the extent that they released the alginate solution, consequently reducing the friction. However, the NaA solution and CaA beads had significant differences in their friction coefficient values at 0.05 m s^{-1} entrainment speeds ($p < 0.05$), which indicates that the beads were not completely destroyed during the tribological shear. It is only when the speed was increased to 0.1 m s^{-1}, no further statistical difference between NaA solution and CaA beads could be noted ($p > 0.05$) (Supplementary Table S1a). Therefore, at such high entrainment speeds, the possibility of the beads bursting and leaching out of the alginate solution from the beads cannot be completely ignored. Another possibility is that the gap between the contact surfaces was sufficiently high in such high entrainment speeds to allow all beads into the gap without compression, reducing their overall influence on the friction behaviour compared to the NaA solution.

3.2. Mechanical characteristics of the hydrogels and the simulated boli

The hydrogels were characterized independently using large deformation rheological tests (puncture and compression test) to mimic the first bite and chewing aspects, while the simulated hydrogel boli were analysed using apparent viscosity measurements and soft tribology analyses to emulate the later part of oral processing (Chen & Stokes, 2012; Krop et al., 2019a; Sarkar et al., 2019b; Stokes et al., 2013).

3.2.1. Textural properties of the hydrogels

The average fracture force and fracture stress of the hydrogels prepared with varying levels of textural complexity (1.67κC+0.33NaA and the three layered 1.67κC+0.33CaA beaded gels) were obtained by puncture tests and compression tests, respectively, and compared to 2κC. It is noteworthy that all hydrogels were composed of the same total biopolymer concentration for comparison purposes (Table 1). The puncture test was performed with a Volodkevitch tooth probe to mimic the first bite-related oral processing properties. Fig. 3a shows a clear difference between the average fracture force for the homogeneous 2κC gel and the four heterogeneous hydrogels, that have either NaA or CaA beads of various sizes incorporated in a layered structure. The 2κC gel has a considerably higher mean puncture force of 4.56 N (±0.28), compared to the remaining four heterogeneous hydrogels in this study ($p < 0.05$). The κC + NaA hydrogel demonstrates the lowest puncture force of 1.29 N (±0.10), whilst all the three layered κC + CaA beaded hydrogels with small, medium and large beads have similar average puncture forces of ~1.4 N, respectively ($p > 0.05$). It is noteworthy that the presence of CaA beads appears to have no impact on the puncture force of the heterogeneous hydrogels as compared to that of the NaA-containing κC hydrogel, which lacks beads ($p > 0.01$).

The compression test, however, in which the sample cut-out is

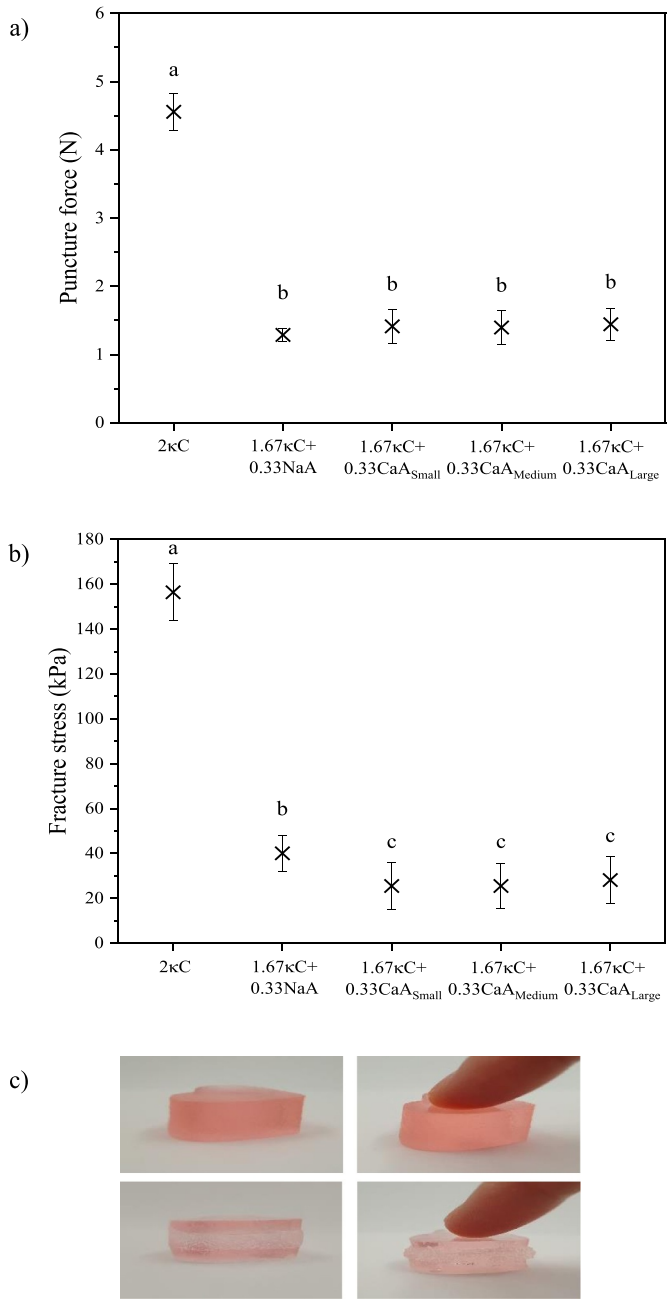

Fig. 3. Mean puncture force (a) and fracture stress (b) obtained using uniaxial puncture and compression tests, respectively, of hydrogels 2κC, 1.67κC+0.33NaA and layered hydrogels 1.67κC+0.33CaA with small, medium and large bead size; and visual images (c) of 1.67κC+0.33NaA (top: without and with pressing with a finger), and layered 1.67κC+0.33CaA hydrogel (bottom: without and with pressing with a finger). Mean was calculated based on at least four measurements performed on three different days. Error bars indicate the standard deviation.

uniaxially compressed with a probe that fully covers the sample, showed a difference between the heterogeneous non-layered κC + NaA and κC + CaA bead layered hydrogels (see Fig. 3b). Noteworthy, the embedding of soft beads to reduce the fracture properties of a semi-solid gel matrix has been also reported elsewhere (Santagiuliana et al., 2018a). Similar to the results of the puncture test, the fracture stress of 2κC was highest (156.39 kPa ±12.80) whilst the κC + NaA and three κC + CaA bead-layered hydrogels had nearly five-times lower average fracture stress ranging from 25 to 40 kPa, respectively ($p < 0.05$). The puncture force and fracture stress of the 2κC hydrogels were in line with previous studies (Krop et al., 2019a; Krop et al., 2019c; Laguna and Sarkar, 2016). Interestingly, unlike the puncture test, the compression test was able to distinguish between the CaA-bead layered hydrogels and the non-beaded mixed gels (κC + NaA) with the addition of the CaA beads resulting in a significantly lower fracture stress as compared to that of the κC + NaA mixed gel ($p < 0.05$). Although one might expect that the fracture stress of the layered and non-layered gels to be similar based on puncture tests results (Fig. 3a), the fracture stress was significantly lower in the CaA beaded-samples (Fig. 3b), most likely due to the expulsion of the beads during the compression (see Fig. 3c). This is in stark contrast to the behaviour observed by Krop et al. (2019a), where κC hydrogels containing CaA beads had a higher fracture stress as compared to the κC + NaA gel of similar total hydrocolloid concentration. This discrepancy might be attributed to the layered structure used in the current gel preparations as opposed to the procedure of dispersing the gel beads on top of κC gels used in the previous study.

In summary, addition of NaA or CaA beads to a κC matrix produces softer hydrogels compared to that of homogeneous κC hydrogel, as shown by their lower puncture forces and fracture stresses. These observations are in line with previous findings by Laguna and Sarkar, 2016, due to segregating interactions between NaA/CaA beads and κC. In the case of κC + NaA hydrogels, addition of NaA, a linear anionic polysaccharide (Braccini & Perez, 2001), interferes with the crosslinking of the κC helices and weakens the overall structure. In the case of the κC + CaA beaded hydrogels, the beads most likely acted as "inactive fillers" or in other words "holes" that were not efficiently bound to the κC matrix (Laguna & Sarkar, 2016), thus reducing both the fracture stress and puncture force in the resultant κC + CaA hydrogels (Fig. 3a and b). Such segregating interactions consequently resulted in local phase separation between the beads and κC layers, as opposed to a single continuous κC gel phase. Instead of the beads binding to the κC hydrogel and improving its resistance to deformation, the lack of interactions between the CaA beads and κC led to the interruption of the κC gel structure and a decrease in its ability to resist the deformation (Ching, Bansal, & Bhandari, 2016). It is worth noting that the texture analyses alone were not able to distinguish the layered hydrogels containing CaA beads of small, medium and large sizes from each other ($p > 0.05$) (Fig. 3a and b). Due to this absence of differences seen in the puncture force and compression fracture stress of the hydrogels with different bead sizes, it appears that the CaA beads acted as inactive fillers within the κC gel matrix, independent of the bead size, as can be observed in the visual images in Fig. 3c, which is expected to be due to the limited interaction between the beads and the κC matrix (Liu, Chan, & Li, 2015).

3.2.2. *Frictional behaviour of the simulated boli*

Friction coefficients of the hydrogel boli and CaA bead boli (without being incorporated into the κC matrix) of different sizes are shown in Fig. 4a and b, respectively. Model saliva acted as the control (Fig. 4a and b), generating the highest friction coefficients as compared to all other bolus samples in the mixed regime ($p < 0.05$) (see Supplementary Table S1 for statistics). Whilst the 2κC, 1.67κC+0.33NaA and 1.67κC+0.33CaA hydrogels with small and medium beads produced very similar mean friction coefficients in the boundary regime ($p > 0.05$, Supplementary Table S1b), the κC + CaA bolus with large beads yielded the lowest friction coefficients in both boundary as well as mixed lubrication regime (at 0.1 m s^{-1} speed) (Fig. 2a, see Supplementary Tables S1b–c for statistics). It is worth noting that in contrast to all other friction curves showing both boundary and mixed lubrication regimes, 1.67κC+0.33CaA$_{Large}$ hydrogel boli showed only mixed lubrication regime (Fig. 4a). No sign of a boundary lubrication regime was observed for this sample even at very low entrainment speeds (<0.005 m s^{-1}) highlighting that this sample could somehow create sufficient surface separation even at such low speeds by the hydrodynamic pressure of the bolus beads (Fig. 4a).

In Fig. 4b, in the boundary regime, the friction coefficients for medium and large-sized CaA beads appeared to be comparable to that of the

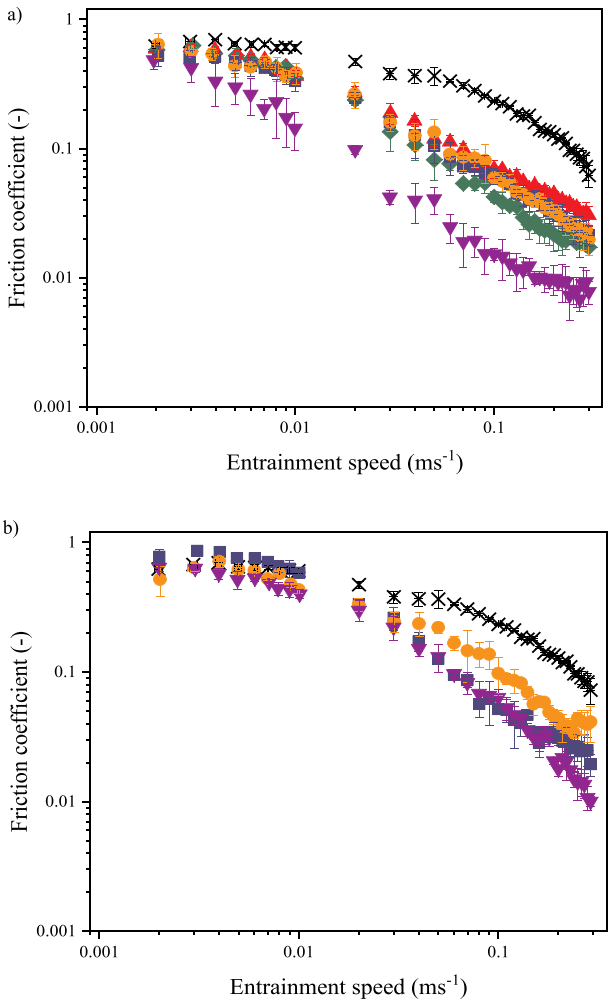

Fig. 4. Mean friction coefficient of the simulated hydrogel boli (a) and simulated beads boli (b) with 2κC (▲), 1.67κC+0.33NaA (♦) and 1.67κC+0.33CaA with small (■), medium (●), and large beads (▼) as a function of entrainment at 37 °C, respectively. The mean was calculated based on at least three replicates. The curve for model saliva (×) was added to both graphs for reference. Error bars show the standard deviation.

model saliva ($p > 0.05$). Interestingly, the friction coefficient of small-sized CaA beads was higher than that of the medium- and large-sized beads ($p < 0.05$) (Supplementary Table S1c). This behaviour of high friction coefficient values can be expected based on Fig. 2, which suggests that the CaA beads were not capable of providing boundary lubrication as they were excluded from the contact region either as beads or as bead boli (Fig. 4b). In the mixed regime, however, the variation between the CaA bead boli and model saliva was more apparent ($p < 0.05$). Interestingly, the boli of the CaA beads did not show any significant difference in their lubrication properties based on size ($p > 0.05$). Compared to the beads on their own without model saliva (Fig. 2), the incorporation of model saliva to form the simulated bolus appeared to be detrimental to the lubricating properties of all the CaA beads leading to higher friction coefficients between the PDMS ball and disc in the mixed regimes in the latter (Fig. 4b). One might argue that the beads might have been destroyed subjected to the tribological shear. As can be seen from the optical microscopy images of the bead boli (see Supplementary Figs. S2a and S2b for CaA_{Small} bead boli and CaA_{Large} bead boli, respectively), the CaA beads were resilient to dissolution in the model saliva, beads were deformed but still clearly discernible in the samples even after subjecting them to the tribological shear.

3.2.3. Apparent viscosity and Stribeck curve of the hydrogel boli

Fig. 5a shows the apparent viscosity of the hydrogel boli beads after simulated oral processing in the presence of model saliva. It can be seen that the viscosity of all the boli decreased upon increasing the shear rates, which is a recognized signature of a shear thinning behaviour. Similar values were also found for the hydrogel boli in our previous study (Krop et al., 2019a). Interestingly, similar to the fracture stress behaviour of the hydrogels (Fig. 3b), the apparent viscosity was similar for the beaded hydrogel boli at orally relevant shear rates of 50 s^{-1} ($p > 0.05$) but the values for the layered hydrogel boli were significantly smaller than the apparent viscosities of non-layered mixed NaA-based hydrogel boli (see Supplementary Table S1d for statistics).

In order to understand the role of the bulk rheological properties on tribology, we calculated the Sommerfeld number to correct for differences in the viscosity of the boli samples. Fig. 5b shows the friction coefficient as function of the product of viscosity (η) and entrainment speed component (U) of the simulated hydrogel boli of 2κC, 1.67κC+0.33NaA, 1.67κC+0.33CaA_{Small} and 1.67κC+0.33CaA_{Large}. The highest shear rate explored in the rheological measurements in this study is 1000 s^{-1} (Fig. 5a). Unfortunately, current procedures available to measure higher shear rate viscosities rely on using narrow gaps (~50 μm) (Davies & Stokes, 2008), which is not suitable for this study owing to the large size of the beads (above 100 μm) contained in the boli. Hence, to plot the Stribeck curves, the high shear rate viscosity value of the 2κC hydrogel boli was used, where the start of the high shear rate plateau was evident (~0.17 Pa s, Fig. 5a).

As it can be seen from Fig. 5b, to arrive at similar friction coefficients

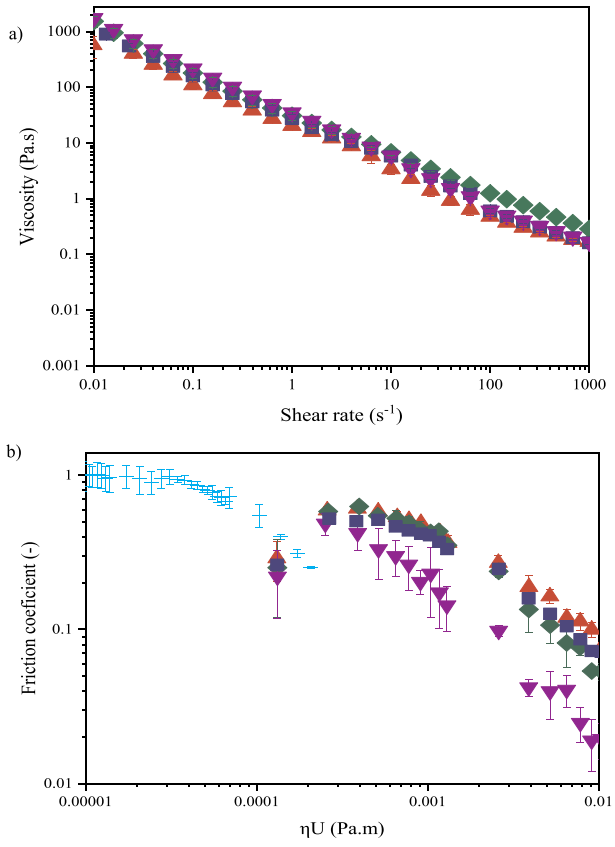

Fig. 5. Viscosity (a) as a function of shear rate at 37 °C and Stribeck master curve (b) as a function of the product of the entrainment speed component (U) and viscosity (η) of the simulated hydrogel boli of 2κC (▲), 1.67κC+0.33NaA (♦) and 1.67κC+0.33CaA with small (■) and large beads (▼), respectively. The curve for MilliQ water (–) was added for reference in (b). The mean was calculated based on at least three replicates. Error bars show the standard deviation.

of μ ~0.5, the ηU component dominating the tribological performance of the boli samples had to be at least one order of magnitude higher in comparison to that of MilliQ water. Although, the second Newtonian plateau viscosity of dispersions of small particles like microgels with hydrodynamic radius around 100 nm (Andablo-Reyes et al., 2019), has been found to dominate the lubrication performance, the large particle size of the beads studied here (in comparison to tribological gaps in the order of hundreds of nanometers to few microns) limits the material entering the gap until the speed is increased. It is also worth noting that 2κC, 1.67κC+0.33NaA and 1.67κC+0.33CaA$_{Small}$ gel boli showed overlapping trends in the Stribeck analysis (Fig. 5b) confirming the role of viscosity in the lubrication phenomena. On the other hand, 1.67κC+0.33CaA$_{Large}$ gel boli continued to demonstrate significantly lower friction coefficient in the 0.001–0.01 Pa m regime as compared to the non-layered and 1.67κC+0.33CaA$_{Small}$ boli (Fig. 5b), indicating that such difference might be perceived in *in vivo* oral conditions.

3.3. Sensory discrimination and perception of texturally complex hydrogels

The results from each of the triangle tests carried out are shown in Table 3, indicating the number of panellists that successfully identified the anomalous gel sample in a set of three (where two were the same and one was different). For a total number of 53 panellists, a minimum of 30 correct answers are needed to establish a significance of $p < 0.001$ (Meilgaard, Civille, & Carr, 2006). When panellists were asked to distinguish between κC + NaA and κC + CaA hydrogels, layered with small, medium or large beads, a high number of correct answers can be observed. In other words, participants were able to correctly identify the different sample at a significant level of $p < 0.001$. However, this was not the case with respect to the two layered hydrogel samples *i.e.* layered 1.67κC+0.33CaA$_{Small}$ versus 1.67κC+0.33CaA$_{Large}$. It was evidently more difficult to distinguish between these two samples with beads, where only 21 participants could identify the odd sample (Table 3). Thus, it can be statistically inferred that participants were not able to distinguish between hydrogels layered with small compared to those with large CaA beads, the former being half the size as compared to the large-sized beads (Fig. 1 a1-c1).

It is now well recognized that the sensory detection of particles depends not only on the size of the particles but also on the particle type, shape, concentration, matrix properties *etc.* (Engelen et al., 2005; Imai, Hatae, & Shimada, 1995). As discussed previously, the modulus of the beads (≤1.0 kPa) (Mahdi et al., 2016) embedded within the κC matrix appeared to be the governing factor; the modulus was extremely low to detect differences between the bead-layered hydrogels based on bead sizes. Also, depending upon the size of the beads, the number of beads within the layered hydrogels would differ. For instance, the number of beads in the 1.67κC+0.33CaA$_{Large}$ layered hydrogels was calculated to be 208 (see diameter in Fig. 1cii) in the 0.56 g bead layer of a single hydrogel cut-out under the assumption that the density of alginate is 1 g cm^{-3}. This is approximately one order of magnitude lower than the number of beads in the 1.67κC+0.33CaA$_{Small}$ hydrogel cut-out (2050 beads, see diameter in diameter Fig. 1aii). Hence, it is also possible that this number of soft beads was not sufficient to identify the difference between these bead-layered hydrogels.

Table 3
Number of correct responses for sensory discrimination test for hydrogels.

Hydrogels	Total number of responses	Number of correct responses	Significant difference
1.67κC + 0.33NaA vs 1.67κC + 0.33CaA$_{Small}$	53	51	$p < 0.001$
1.67κC + 0.33NaA vs 1.67κC + 0.33CaA$_{Medium}$	53	46	$p < 0.001$
1.67κC + 0.33NaA vs 1.67κC + 0.33CaA$_{Large}$	52	45	$p < 0.001$
1.67κC + 0.33CaA$_{Small}$ vs 1.67κC + 0.33CaA$_{Large}$	60	21	$p > 0.05$

Fig. 6 shows the intensity ratings (see Supplementary Fig. S3 for gel-wise sensory attributes) and Table 4 shows the Pearson's correlation in order to check for inter-relationships between the sensory textural attributes. The comparison of the samples with respect to each attribute is described as follows:

Hard. As can be seen in Fig. 6, the mixed non-layered 1.67κC+0.33NaA was rated to be less hard than the layered hydrogels (1.67κC+0.33CaA - small, medium and large) ($p < 0.05$). However, the bead-layered samples of different sizes were perceived by the untrained panellists as having the same level of hardness ($p > 0.05$).

Chewy. With regards to chewiness, similar results to the hardness can be noted, which is corroborated by a high correlation between the attributes, "chewy" and "hard" attributes (Table 4). The κC + NaA hydrogel was perceived significantly less chewy than the layered samples ($p < 0.05$) (Fig. 6).

Consistent with a study by Larsen, Tang, Ferguson, Morgenstern, and James (2016b), where the more complex gels (heterogeneous) were perceived as harder and chewier, the layered gels (with higher degree of complexity) were rated with a high score on hardness and chewiness. This might be attributed to the fact that participants were most likely rating the top and bottom layers of the κC + CaA gels (with small, medium and large beads size), comprising of 2.5 wt% κC, which were hard and chewy in comparison to the κC + NaA hydrogels.

Smooth and Slippery. Participants identified 'smooth' samples as 'slippery' and vice versa as can be inferred from the high correlation coefficients between these two attributes (Table 4). There was no significant difference between the layered and non-layered samples (Fig. 6) ($p > 0.05$). It can be observed that the layered gel with CaA beads of medium size was scored slightly higher than the rest of the samples, however this was not significantly different.

Pasty. In terms of pastiness, 1.67κC+0.33NaA was perceived to be significantly pastier than the layered 1.67κC+0.33CaA$_{Medium}$ (Fig. 6). Interestingly, the attribute 'pasty' was found to be inversely correlated with hard, chewy ($p < 0.05$) and 'smooth' ($p < 0.01$) (Table 4). Consequently, the bead-layered gels were perceived to less pasty than the non-layered hydrogels ($p < 0.05$).

Gritty. It is noteworthy that 'gritty' was highly correlated with the

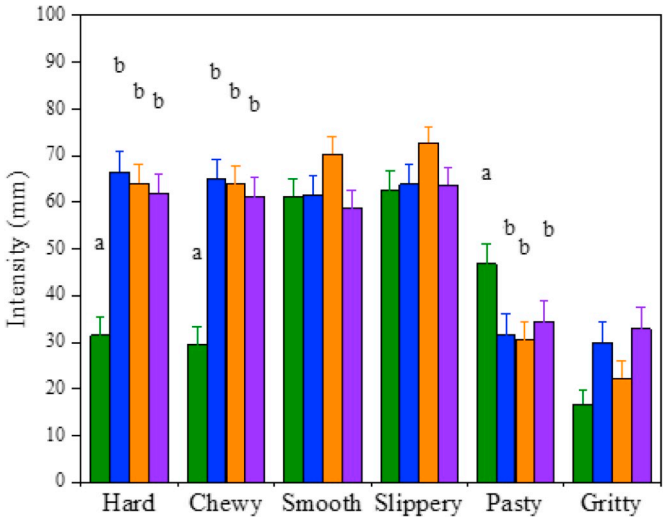

Fig. 6. The intensity ratings of the sensory attributes for 1.67κC+0.33NaA (■), 1.67κC+0.33CaA$_{Small}$ (■), 1.67κC+0.33CaA$_{Medium}$ (■) and 1.67κC+0.33CaA$_{Large}$ (■) with respect to the reference sample (2κC). Data points represent the mean intensity ratings of untrained panellists (n = 60). Error bars indicate the standard error of mean and different lowercase letters represent a statistically significant difference ($p < 0.05$).

Table 4
Pearson's correlations between sensory attributes of the hydrogels. Green colour indicates positive and red colour a negative correlation with $p < 0.05$ in light colours and $p < 0.01$ in the darker shade.

	Hard	Chewy	Smooth	Slippery	Pasty	Gritty
Hard	1	.854**	.420**	.381**	-.268**	0.032
Chewy	0.854**	1	.412**	.432**	-.210**	0.051
Smooth	0.420**	0.412**	1	.719**	-.155*	-.238**
Slippery	0.381**	0.432**	0.719**	1	-0.065	-.197**
Pasty	-0.268**	-0.210**	-0.155*	-0.065	1	.487**
Gritty	0.032	0.051	-0.238**	-0.197**	0.487**	1

'pasty attribute' and thus negatively correlated with 'smooth' and 'slippery' (Table 4). With regards to grittiness, even the κC + NaA mixed hydrogel was perceived as gritty (Supplementary Fig. S3) with respect to the reference (2κC) and it can be noted that there was no significant difference between non-layered and bead-layered samples ($p > 0.05$) (Fig. 6). Similar to a study by Santagiuliana et al. (2018a), it can be suggested that increased particle size can cause heterogeneous sensations in the perception of food.

Overall, it can be concluded that participants were able to distinguish easily between layered and non-layered hydrogels, but not within the layered gels with small bead size when compared to that of the large bead size.

3.4. Explanation of sensory characteristics of hydrogels using instrumental characteristics

There is increasing evidence now on relating instrumental textural measurements to sensory perception, yet most of these studies are carried out with trained panellists (Pradal et al., 2016; Prakash, Tan, & Chen, 2013; Sarkar et al., 2019b; Shewan, Pradal, & Stokes, 2019). In this study, compression tests (Fig. 3b) revealed that mixed hydrogels (κC + NaA) required significantly more force to be broken down as compared to the layered gels, which is exactly opposite to what was revealed by the untrained participants with layered gels being perceived to be significantly 'harder' and 'chewier' as compared to the mixed gels (Fig. 6). Therefore, this indicates that humans may perceive or evaluate food texture, particularly in case of layered hydrogels, differently compared to large deformation measurements. Of more importance here is that the role of saliva during *in vivo* oral processing of the samples that cannot be ignored, and saliva was not included in the compression test. In addition, the missing link between uniaxial compression and perceived texture could be due to the heterogeneous structure of the model foods used in this study. unlike the previously studied homogenous gels (Çakır et al., 2012; Devezeaux de Lavergne et al., 2015; Krop et al., 2019a), where the relation between uniaxial compression tests and sensory perception is well recognized. More specifically, current results might be linked to the top and bottom κC layers in the κC + CaA bead-layered hydrogels that were perceived to be harder by the participants than the κC + NaA hydrogels during the first compression between tongue and palate.

Noteworthy is that although 'smooth' and 'slippery' can be important lubrication-related attributes that can distinguish fat-based samples (Kokini, Kadane, & Cussler, 1977; Upadhyay & Chen, 2019), they can be difficult to understand in non-fat hydrogel samples (Fig. 6 and Supplementary Fig. S3) and thus were not a differentiating factor between current samples, which was also observed even with a trained panel in our previous study with hydrogels (Krop et al., 2019a). Interestingly, both Figs. 2 and 4a show high lubricity behaviour for the large-sized beads irrespective of them being on their own or as simulated hydrogel boli in the mixed regime. One should then expect that the high lubricating capacity of the large beads would result in lower perceived grittiness, which is not the case as shown in Fig. 6. These results might be attributed to the much higher contact pressures existing in a tribometer with PDMS tribopairs as compared to the tongue-palate contact pressures (Sarkar et al., 2019a). The *in vitro* tribological experiments might have allowed squeezing out the alginate solution to create a 'hydrating layer' separating the surfaces as discussed in previous sections (Fig. 2, Supplementary Table S1). In contrast, in a real oral processing scenario during *in vivo* sensory evaluation by consumers, the pressures might be reasonably low; proving insufficient to break these beads down to a hydrating biopolymeric layer. Consequently, these large beads were perceived as 'particles' described by higher perceived 'gritty' intensity.

4. Conclusions

In this study, instrumental methods were used to quantify differences in textural complexities of layered hydrogels for the first time by incorporating a monolayer of soft beads of different sizes in the gel network and we aimed to determine whether such instrumental differences (if any) could then be sensorially perceived by untrained panellists. In this study, neither fracture stress of the hydrogels nor apparent viscosity of the hydrogel boli at orally relevant shear rate could statistically distinguish the layered hydrogels based on bead size. On the other hand, soft tribology analysis of beads as well as the hydrogel boli containing beads could successfully discriminate the large-sized beads from the smaller-sized beads in the mixed lubrication regime. Although textural differences between the mixed (NaA) and the three CaA beaded carrageenan hydrogels were sensorially perceived, participants were unable to distinguish the beaded samples in the present study based on bead size, which can be attributed to the low modulus of the beads used in these layered hydrogels. Overall, this study has important implications for generating novel texture by incorporating soft beads as a layer in hydrogels, where the presence of soft beads can generate distinguishing textural features versus non-beaded hydrogels that can be perceived by consumers.

Declaration of competing interest

None.

CRediT authorship contribution statement

Ecaterina Stribiţcaia: Writing - original draft, Methodology, Validation, Formal analysis, Investigation, Data curation, Writing - review & editing, Visualization, Project administration. **Emma M. Krop:** Methodology, Formal analysis, Data curation, Writing - review & editing, Visualization, Supervision. **Rachel Lewin:** Formal analysis, Investigation. **Melvin Holmes:** Formal analysis, Software, Writing - review & editing, Validation. **Anwesha Sarkar:** Conceptualization, Writing - review & editing, Visualization, Supervision, Funding acquisition.

Acknowledgements

This study has received funding from the European Research Council (ERC) under the European Union's Horizon 2020 research and innovation programme (grant agreement n° 757993).

Appendix A. Supplementary data

Supplementary data to this article can be found online at https://doi.org/10.1016/j.foodhyd.2020.105692.

The data presented in this article will be openly available from the University of Leeds data repository: https://doi.org/10.5518/769.

References

Andablo-Reyes, E., Yerani, D., Fu, M., Liamas, E., Connell, S., Torres, O., et al. (2019). Microgels as viscosity modifiers influence lubrication performance of continuum. *Soft Matter, 15*(47), 9614–9624.

Braccini, I., & Perez, S. (2001). Molecular basis of C(2+)-induced gelation in alginates and pectins: The egg-box model revisited. *Biomacromolecules, 2*(4), 1089–1096.

Çakır, E., Daubert, C. R., Drake, M. A., Vinyard, C. J., Essick, G., & Foegeding, E. A. (2012). The effect of microstructure on the sensory perception and textural characteristics of whey protein/κ-carrageenan mixed gels. *Food Hydrocolloids, 26*(1), 33–43.

Chen, J., & Stokes, J. R. (2012). Rheology and tribology: Two distinctive regimes of food texture sensation. *Trends in Food Science & Technology, 25*(1), 4–12.

Ching, S. H., Bansal, N., & Bhandari, B. (2016). Rheology of emulsion-filled alginate microgel suspensions. *Food Research International, 80*, 50–60.

Davies, G., & Stokes, J. (2008). Thin film and high shear rheology of multiphase complex fluids. *Journal of Non-newtonian Fluid Mechanics, 148*(1–3), 73–87.

Devezeaux de Lavergne, M., van de Velde, F., van Boekel, M. A. J. S., & Stieger, M. (2015). Dynamic texture perception and oral processing of semi-solid food gels (part 2): Impact of breakdown behaviour on bolus properties and dynamic texture perception. *Food Hydrocolloids, 49*, 61–72.

Engelen, L., Van der bilt, A., Schipper, M., & Bosman, F. (2005). Oral size perception of particles: Effect of size, type, viscosity and method. *Journal of Texture Studies, 36*(4), 373–386.

Gabriele, A., Spyropoulos, F., & Norton, I. T. (2010). A conceptual model for fluid gel lubrication. *Soft Matter, 6*(17), 4205–4213.

Hashmi, S. M., & Dufresne, E. R. (2009). Mechanical properties of individual microgel particles through the deswelling transition. *Soft Matter, 5*(19), 3682–3688.

Imai, E., Hatae, K., & Shimada, A. (1995). Oral perception of grittiness: Effect of particle size and concentration of the dispersed particles and the dispersion medium. *Journal of Texture Studies, 26*(5), 561–576.

Kokini, J. L., Kadane, J. B., & Cussler, E. L. (1977). Liquid texture perceived in the mouth. *Journal of Texture Studies, 8*(2), 195–218.

Krop, E. M., Hetherington, M. M., Holmes, M., Miquel, S., & Sarkar, A. (2019a). On relating rheology and oral tribology to sensory properties in hydrogels. *Food Hydrocolloids, 88*, 101–113.

Krop, E. M., Hetherington, M. M., Miquel, S., & Sarkar, A. (2019b). The influence of oral lubrication on food intake: A proof-of-concept study. *Food Quality and Preference, 74*, 118–124.

Krop, E. M., Hetherington, M. M., Miquel, S., & Sarkar, A. (2019c). Oral processing of hydrogels: Influence of food material properties versus individuals' eating capability. *Journal of Texture Studies*.

Krop, E. M., Hetherington, M. M., Nekitsing, C., Miquel, S., Postelnicu, L., & Sarkar, A. (2018). Influence of oral processing on appetite and food intake – a systematic review and meta-analysis. *Appetite, 125*, 253–269.

Laguna, L., Hetherington, M. M., Chen, J., Artigas, G., & Sarkar, A. (2016a). Measuring eating capability, liking and difficulty perception of older adults: A textural consideration. *Food Quality and Preference, 53*, 47–56.

Laguna, L., & Sarkar, A. (2016). Influence of mixed gel structuring with different degrees of matrix inhomogeneity on oral residence time. *Food Hydrocolloids, 61*, 286–299.

Larsen, D. S., Tang, J., Ferguson, L. R., & James, B. J. (2016). Increased textural complexity in food enhances satiation. *Appetite, 105*, 189–194.

Larsen, D. S., Tang, J., Ferguson, L. R., Morgenstern, M. P., & James, B. J. (2016). Oral breakdown of texturally complex gel-based model food. *Journal of Texture Studies*.

Liu, S., Chan, W. L., & Li, L. (2015). Rheological properties and scaling laws of κ-carrageenan in aqueous solution. *Macromolecules, 48*(20), 7649–7657.

Liu, K., Tian, Y., Stieger, M., van der Linden, E., & van de Velde, F. (2016). Evidence for ball-bearing mechanism of microparticulated whey protein as fat replacer in liquid and semi-solid multi-component model foods. *Food Hydrocolloids, 52*, 403–414.

Mahdi, M. H., Diryak, R., Kontogiorgos, V., Morris, G. A., & Smith, A. M. (2016). In situ rheological measurements of the external gelation of alginate. *Food Hydrocolloids, 55*, 77–80.

Meilgaard, M., Civille, G. V., & Carr, B. T. (2006). *Sensory evaluation techniques*. CRC Press.

Nemenyi, P. (1963). *Distribution-free multiple comparisons. unpublished Ph. D*. Ph. D. Dissertation, thesis. Princeton, New Jersey: Princeton University.

Pradal, C., & Stokes, J. R. (2016). Oral tribology: Bridging the gap between physical measurements and sensory experience. *Current Opinion in Food Science, 9*, 34–41.

Prakash, S., Tan, D. D. Y., & Chen, J. (2013). Applications of tribology in studying food oral processing and texture perception. *Food Research International, 54*(2), 1627–1635.

R Core Team. (2018). *R: A language and environment for statistical computing*. Vienna, Austria: R Foundation for Statistical Computing. http://www.R-project.org/.

Santagiuliana, M., Christaki, M., Piqueras-Fiszman, B., Scholten, E., & Stieger, M. (2018a). Effect of mechanical contrast on sensory perception of heterogeneous liquid and semi-solid foods. *Food Hydrocolloids, 83*, 202–212.

Santagiuliana, M., Marigómez, I. S., Broers, L., Hayes, J. E., Piqueras-Fiszman, B., Scholten, E., et al. (2019). Exploring variability in detection thresholds of microparticles through participant characteristics. *Food & Function, 10*(9), 5386–5397.

Santagiuliana, M., Piqueras-Fiszman, B., van der Linden, E., Stieger, M., & Scholten, E. (2018b). Mechanical properties affect detectability of perceived texture contrast in heterogeneous food gels. *Food Hydrocolloids, 80*, 254–263.

Sarkar, A. (2019). Oral processing in elderly: Understanding eating capability to drive future food texture modifications. *Proceedings of the Nutrition Society, 78*(3), 329–339.

Sarkar, A., Andablo-Reyes, E., Bryant, M., Dowson, D., & Neville, A. (2019a). Lubrication of soft oral surfaces. *Current Opinion in Colloid & Interface Science, 39*, 61–75.

Sarkar, A., Goh, K. K. T., & Singh, H. (2009). Colloidal stability and interactions of milk-protein-stabilized emulsions in an artificial saliva. *Food Hydrocolloids, 23*(5), 1270–1278.

Sarkar, A., Kanti, F., Gulotta, A., Murray, B. S., & Zhang, S. (2017). Aqueous lubrication, structure and rheological properties of whey protein microgel particles. *Langmuir, 33*(51), 14699–14708.

Sarkar, A., & Krop, E. M. (2019b). Marrying oral tribology to sensory perception: A systematic review. *Current Opinion in Food Science*.

Sarkar, A., Xu, F., & Lee, S. (2019c). Human saliva and model saliva at bulk to adsorbed phases – similarities and differences. *Advances in Colloid and Interface Science, 273*, 102034.

Shewan, H. M., Pradal, C., & Stokes, J. R. (2019). Tribology and its growing use toward the study of food oral processing and sensory perception. *Journal of Texture Studies*, 1–16.

Stokes, J. R., Boehm, M. W., & Baier, S. K. (2013). Oral processing, texture and mouthfeel: From rheology to tribology and beyond. *Current Opinion in Colloid & Interface Science, 18*(4), 349–359.

Strand, K. A., Bøe, A., Dalberg, P. S., Sikkeland, T., & Smidsrød, O. (1982). Dynamic and static light scattering on aqueous solutions of sodium alginate. *Macromolecules, 15*(2), 570–579.

Tang, J., Larsen, D. S., Ferguson, L. R., & James, B. J. (2016). The effect of textural complexity of solid foods on satiation. *Physiology & Behavior, 163*, 17–24.

Torres, O., Tena, N. M., Murray, B., & Sarkar, A. (2017). Novel starch based emulsion gels and emulsion microgel particles: Design, structure and rheology. *Carbohydrate Polymers, 178*, 86–94.

Torres, O., Yamada, A., Rigby, N. M., Hanawa, T., Kawano, Y., & Sarkar, A. (2019). Gellan gum: A new member in the dysphagia thickener family. *Biotribology, 17*, 8–18.

Tyle, P. (1993). Effect of size, shape and hardness of particles in suspension on oral texture and palatability. *Acta Psychologica, 84*(1), 111–118.

Upadhyay, R., & Chen, J. (2019). Smoothness as a tactile percept: Correlating 'oral' tribology with sensory measurements. *Food Hydrocolloids, 87*, 38–47.

Utz, K. H. (1986). The interocclusal tactile fine sensitivity of the natural teeth as studied by aluminum oxide particles. *Deutsche Zahnarztliche Zeitschrift, 41*(3), 313–315.

de Wijk, R. A., & Prinz, J. F. (2005). The role of friction in perceived oral texture. *Food Quality and Preference, 16*(2), 121–129.